PAPER

Check for updates

Water and mildew proof SiO$_2$ & ZnO/silica sol superhydrophobic composite coating on a circuit board†

Ziang Li,[a] Changquan Li, [iD] *[a] Junfei Ou, [iD] *[a] Xinzuo Fang,[a] Mengqi Cong,[a] Chen Wang,[a] Feifei Mao,[a] Tianci Mao[a] and Alidad Amirfazli [iD] [b]

In order to improve the waterproof and mildew resistance of electronic equipment, a superhydrophobic coating was prepared on a circuit board. First, hexadecyl trimethoxysilane was used to modify the nano silica and nano zinc oxide particles, and then the modified nanoparticles were mixed with the silica sol. Then the superhydrophobic coating was prepared on the surface of the printed circuit board by a spraying process. The preparation technology and physical and chemical properties of the coating were studied. The contact angle of the final sample can reach 169.47°, the sliding angle can reach 1.2°, it has good acid and alkali corrosion resistance, resistance to NaCl, self-cleaning performance and antimildew performance.

1. Introduction

Electronic equipment will be covered by some dust in the process of use, and some special electronic equipment is used in acid–base, seawater and humid environments, so these external factors will seriously affect the heat dissipation and service life of the circuit board.[1–3] At present, although some circuit board protective adhesives can achieve water and corrosion resistance, there are still some problems, for example, the self-cleaning and antimildew performance of the coating is poor, which increases the failure rate of electronic products and reduces the service life of electronic products.

A superhydrophobic surface means that the contact angle between the water droplet and the contact surface is greater than 150° and the sliding angle is less than 10° at the same time. The water droplet will remain spherical on the superhydrophobic surface and roll easily,[4,5] therefore, superhydrophobicity has great potential application value in waterproofing, self-cleaning, corrosion resistance and other aspects,[6–16] but rarely reported in electronic products such as circuit boards. There are two key factors to construct superhydrophobic surface: one is that the surface has a certain roughness, the other is that the surface has a low surface energy.[17,18] In nature, the appearance of the muddy lotus and the rolling water droplets on the lotus leaf are the result of the special structure on its surface.[19,20] Based on the above two key factors, scientists have explored a number of methods for preparing super hydrophobic surfaces: sol–gel, layer by layer self-assembly, surface etching, electrospinning, film forming, vapor deposition, *etc.*[21–27] Sol–gel method has many advantages, such as easy control of reaction process, high uniformity of coating and wide application of substrate. For example, Wang *et al.*,[3] a fluorinated silica sol based super hydrophobic coating was prepared on the printed circuit board by sol–gel method. The contact angle of the coating was 158°, the sliding angle is 3°. Yang *et al.*,[28] the superhydrophobic coating of fluorinated functionalized titanium dioxide sol was prepared on the surface of cotton fabric by sol–gel method. The contact angle of samples was 160°.

In this paper, silica sol was prepared by sol–gel method, and then the different particle size of SiO$_2$ & ZnO modification, then the superhydrophobic composite coating was prepared by mixing silica sol and modified nanoparticles. The effects of the mass ratio of silica to zinc oxide, the mass ratio of surface modifier to nanoparticles, and the mass ratio of nanoparticles to silica sol on the hydrophobicity of the coating were investigated, and the microstructure of the coating was characterized. The chemical and mechanical durability of superhydrophobic coatings, such as acid and alkali corrosion resistance, friction resistance and mildew resistance, were studied.

2. Experimental

2.1. Materials

Tetraethyl orthosilicate (TEOS) was purchased at Guangzhou Wengjiang Chemical Reagent Co., Ltd. Hexadecyl trimethoxysilane (HDTMS, mass fraction of 85%) was obtained at Shanghai McLean Biochemical Technology Co., Ltd. Sodium

[a]School of Materials and Engineering, Jiangsu University of Technology, Changzhou, Jiangsu, 213001, People's Republic of China. E-mail: 498024540@qq.com; oujunfei_1982@163.com

[b]Department of Mechanical Engineering, York University, Toronto, ON, M3J 1P3, Canada

† Electronic supplementary information (ESI) available: A table of contents entry and antibacterial test report. See DOI: 10.1039/d1ra03140f

chloride (NaCl), sodium hydroxide (NaOH), hydrochloric acid (HCl), anhydrous ethanol and ammonia water are all analytical pure, all of which are purchased from Guoyao Group Chemical Reagent Co., Ltd. SiO_2 (100 nm particle size) was purchased from Hebei Bocheng Metallurgical Research Center. ZnO (30 nm particle size) was produced by Guangzhou Changyu Chemical Technology Co., Ltd. The circuit board (PCB, green, single side, 3×5 cm) was purchased from Shenzhen Kebi micro Semiconductor Co., Ltd.

2.2. Preparation of superhydrophobic nanocomposite coatings

2.2.1. Preparation of silica sol. 75 ml absolute ethanol, 10 ml deionized water and 3 ml ammonia water were added into the beaker and stirred evenly at the speed of 500 rpm, then 6 ml TEOS was added slowly and stirred continuously at the speed of 500 rpm for 3 h to obtain silica sol.[29]

2.2.2. Hydrophobic modification of nanoparticles. SiO_2 and ZnO nanoparticles were added into the mixed solvent of anhydrous ethanol and deionized water, a certain amount of HDTMS was added and stirred at the speed of 600 rpm for 5 h to obtain the modified material SiO_2 & ZnO solution.

2.2.3. Preparation of superhydrophobic nanocomposite coatings. A certain amount of hydrophobically modified nanoparticle solution was added to 15 ml silica sol, and 30 min was prepared by emulsion stirring. The emulsion was sprayed onto the surface of the clean PCB by spraying. The specific spraying process is as follows: adjust the relative pressure of the air pump to 2 bar, adjust the distance between the muzzle of the spray gun and the PCB to 10 cm, spray slowly on the circuit board with Z-shaped technique, and dry at room temperature for 5 h after spraying. As shown in Fig. 1.

2.3. Characterization of structure and wettability

The molecular structure of hydrophobic modified nanoparticles was analyzed by FTIR (Nicolet is 5). The microstructure of superhydrophobic composite coating was analyzed by SEM (QUANTA FEG 400). Surface element analysis of superhydrophobic composite coating by EDS (Genesis). The wettability of the sample was measured by optical contact angle instrument (Kruss, DSA30), the volume of water droplet was 10 µl, the test was repeated at five different positions of the sample, and the average value was taken as the test value.
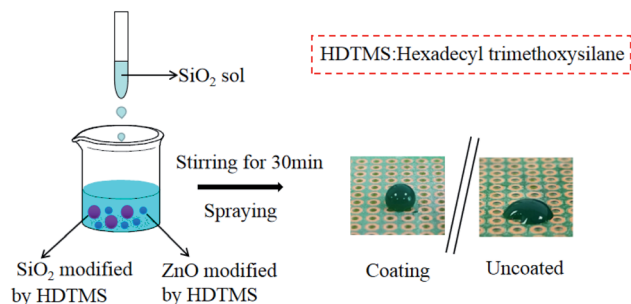

Fig. 1 Preparation of superhydrophobic coating.

2.4. Performance testing

2.4.1. Corrosion resistance. The samples were immersed in aqueous solutions with different pH values or NaCl (3.5 wt%) aqueous solutions, wash and dry with water every other time, then test the wetting performance of the sample and record the change of wettability on the surface of the sample.

2.4.2. Electrochemical test. The electrochemical impedance spectrum of the sample was measured by the electrochemical workstation (Gamry reference 3000), the sample, AgCl electrode and Pt electrode correspond to working electrode, reference electrode and counter electrode respectively. The exposed area of the sample is 1 cm^2, and the corrosion medium is 3.5 wt% NaCl aqueous solutions.

2.4.3. Friction resistance test. Place the sample (15 cm^2) on 800 mesh sandpaper and load 50 g weight, push it back and forth horizontally, the speed is about 5 cm s^{-1}, 10 cm at a time, the surface wettability of the sample was recorded every 10 times.[30]

2.4.4. Mildew resistance. The powdery mildew resistance was assessed in obedience to GB/T2423.16-2008 standard for environmental testing of electrical and electronic products, the sample was inoculated with a spore suspension by spraying and cultured at the temperature (29 ± 1) °C and the relative humidity (90–100%). The mildew growth of the sample was afterwards observed within 28 days.

2.4.5. Self cleaning. The cement powder is evenly spread on the surface of the superhydrophobic PCB and pristine PCB, observe the situation of water drops rolling away dust.

3. Results and discussion

3.1. Influencing factors of coating wettability

3.1.1. Influence of preparation process. There are two key factors to construct superhydrophobic surface, surface roughness and low surface energy. In this paper, the micro–nano rough structure is constructed by using SiO_2 and ZnO with different particle sizes, the influence of mass ratio of SiO_2 to ZnO on the hydrophobicity of the coating was investigated, the test results of contact angle and sliding angle are shown in Fig. 2(A). At this time, the mass ratio of surface modifier to nano particle is 3%, the mass ratio of nanoparticles to silica sol is 3%. It can be seen from Fig. 2(A) that the contact angle is 164° and the sliding angle is 8.2° when SiO_2 is used alone. The contact angle is 167.5° and the sliding angle is 10.3° when ZnO is used alone. When SiO_2 and ZnO are mixed, with the increase of ZnO content, the SiO_2 content decreases, and the contact angle basically remains stable, while the sliding angle first decreases and then increases, this is because the mixed use of nanoparticles with different sizes can better construct the rough structure. Fig. 3(a) and (c) shows the SEM picture of SiO_2 and ZnO with mass ratio of 1 : 0, Fig. 3(b) and (d) are SEM images of SiO_2 and ZnO with mass ratio of 1 : 1. It can be seen from Fig. 3(a)–(d) that the surface with the mass ratio of SiO_2 to ZnO of 1 : 1 is coarser than the surface with the mass ratio of SiO_2 to ZnO of 1 : 0, and has the micro–nano rough structure required for superhydrophobic surface. When the two nanoparticles are
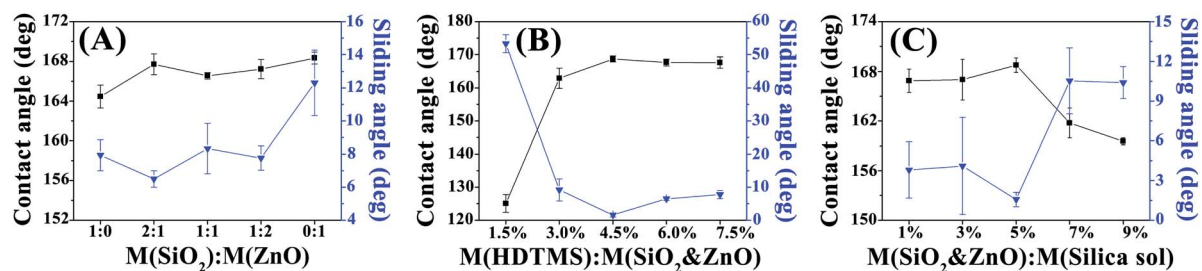
Fig. 2 The effect of SiO2 and ZnO quality ratio on hydrophobicity of coating (A); the effect of mass ratio of surface modifier and nanoparticles on hydrophobicity of coating (B); the effect of the mass ratio of nano particles and silica sol on hydrophobic properties of coating (C).
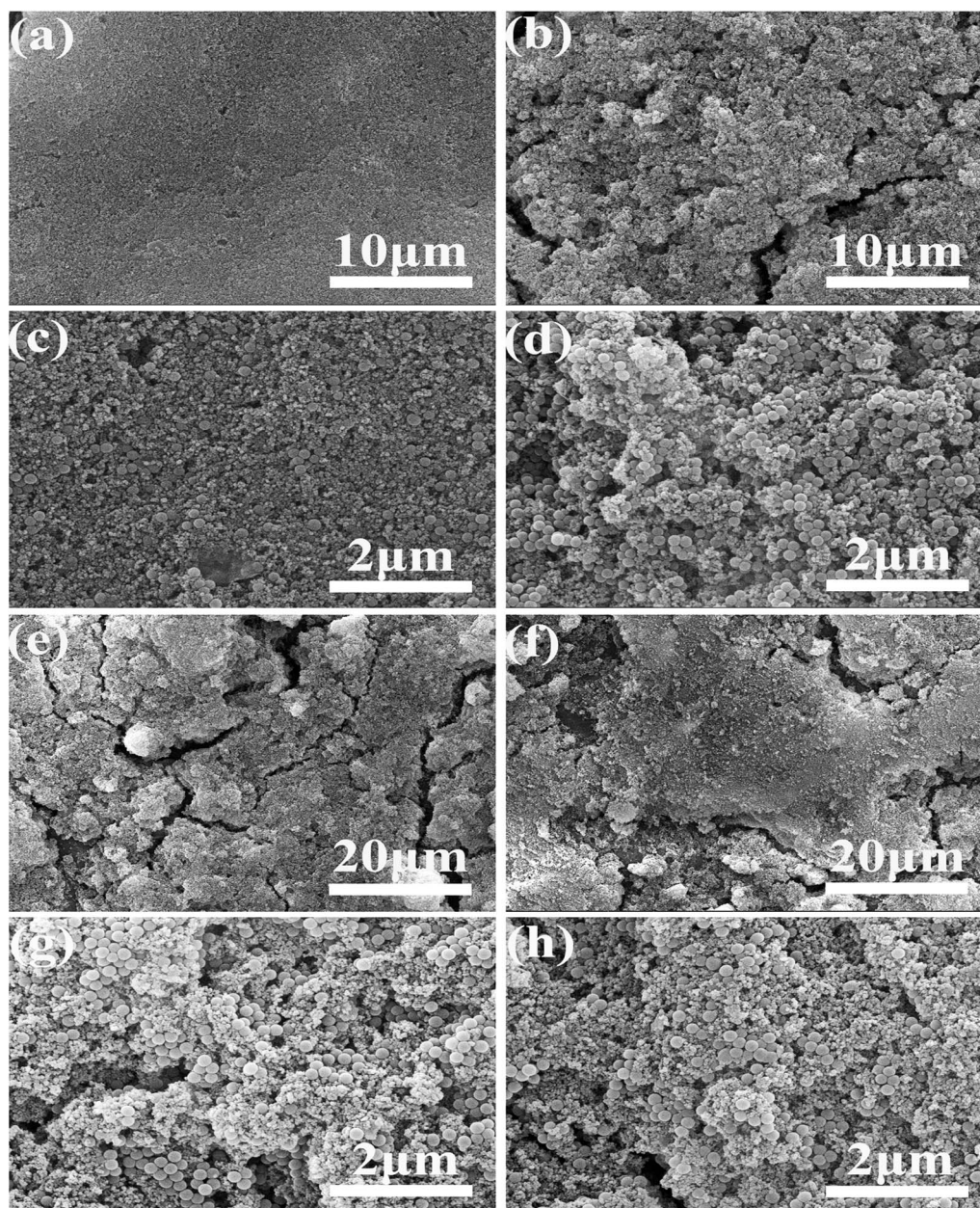

Fig. 3 SEM images of different samples. SEM with mass ratio of SiO2 to ZnO 1 : 0 (a and c); SEM with mass ratio of SiO2 to ZnO 1 : 1 (b and d); SEM with 1% mass ratio of nano particles to silica sol (e and g); SEM with 1% mass ratio of nano particles to silica sol (f and h).

mixed, the hydrophobicity of the coating has little change, this is because when the surface roughness of the coating reaches a certain level, the surface energy of the coating surface plays a very important role.

The mass ratio of SiO_2 to ZnO is 2 : 1 and the mass ratio of nano particle to silica sol is 3%, other production processes remain unchanged, the effect of the mass ratio of surface modifier to nanoparticles on the hydrophobicity of the coating was investigated, the test results of contact angle and sliding angle are shown in Fig. 2(B). As can be seen from Fig. 2(B), when the mass ratio of HDTMS to nanoparticles is 1.5%, the contact angle is 121° and the sliding angle is 58.3° and the super-hydrophobic effect cannot be achieved. With the increase of HDTMS content, the contact angle increases and the sliding angle decreases. When the content of HDTMS is 4.5%, the maximum contact angle is 168.3° and the sliding angle is 4.3° lower. With the increase of HDTMS content, the stronger the ability of nanoparticles to resist hydrophilic groups, the smaller the surface energy and the stronger the hydrophobicity of the coating. After adding HDTMS, the contact angle and sliding angle remained stable, this is because the surface energy of the surface is difficult to continue to decrease when it is low to a certain extent, considering the economic and practical effects, the mass ratio of HDTMS to nanoparticles is 4.5%.

The mass ratio of SiO_2 to ZnO is 2 : 1, the mass ratio of HDTMS to nanoparticles is 4.5%, and other processes remain unchanged, the influence of the mass ratio of nano particles to silica sol on the hydrophobicity of the coating is explored. The test results of contact angle and sliding angle are shown in Fig. 2(C). As can be seen from Fig. 2(C). When the mass ratio of nanoparticles to silica sol is 1%, the contact angle and sliding angle are 168.2° and 3.2°. When the mass ratio of nanoparticles to silica sol is 5%, the contact angle is 169.47° and the sliding angle is 1.2°. At this stage, with the increase of the amount of nanoparticles, the hydrophobicity of the coating becomes better, this is due to the increase of nanoparticles, the structure of a better rough structure. When the mass ratio of nano particles to silica sol increases to 9%, the contact angle is 158.9° and the sliding angle is 9.7° and the hydrophobicity of the coating decreases, the reason is that the content of silica sol decreases, resulting in a large number of nanoparticles cannot adhere to the coating surface, and cannot create a better rough structure, so the hydrophobicity of the coating decreases.

Fig. 3(e) and (g) shows SEM with 1% mass ratio of nanoparticles to silica sol, and Fig. 3(f) and (h) shows SEM with a mass ratio of 9% between nanoparticles and silica sol. Compared with the low power mirror (e and f), it can be found that the sample with mass ratio of 1% adheres more coatings on the surface, so it has better hydrophobicity.

3.1.2. Influence of surface chemical composition and morphology.

The FTIR spectra of HDTMS, SiO_2, ZnO and their mixed modified nanoparticles are shown in Fig. 4(A). The absorption peak arising in the spectrum of modified nano-particles at 3353.05 cm^{-1} is attributed to stretching and bending vibrations of hydroxyl or bridged hydroxyl groups as a result of dissociation of a large number of water molecules on the surface of nano-SiO_2 and ZnO.[31] In Fig. 4(A), spectral line a is compared with spectral lines c and d, 2976.93 cm^{-1} and 2910.86 cm^{-1} is the stretching vibration peak of –CH_3 and –CH_2, this indicates that HDTMS is successfully grafted on nanoparticles. The absorption peak at 1646.97 cm^{-1} is the water content in potassium bromide. The peak at 1381.42 cm^{-1} is the vibration generated by ester group (–COOR) radicals of a coupling agent. Those at 1086.78 cm^{-1} and 1043.27 cm^{-1} are brought by the anti-symmetric and symmetric contraction vibrations of Si–O–Si bonds.[32] Finally, the signature at 879.15 cm^{-1} refers to the contraction vibration of Zn–O bonds that are formed by the dehydration reaction between HDTMS hydrolyzed to Si–OH and –OH radicals on the SiO_2 and ZnO surfaces, as shown in Fig. 4(B).[33]

Fig. 5 SEM of pristine PCB surface, it can be seen from the low power Fig. 5(a) that there are some rough structures arranged disorderly on the surface of the pristine PCB, however, in the high power Fig. 5(c), the surface is smooth and there is no obvious rough structure, which indicates that the surface of the untreated circuit board has no rough structure needed to construct superhydrophobic surface. SEM of superhydrophobic PCB surface (d–f), in the low power Fig. 5(d), it can be seen that there are many synaptic nanoparticles on the surface of the sample, which are densely and neatly arranged on the surface, this is a micro–nano rough structure composed of hydro-phobically modified nanoparticles added into the coating, in the high power Fig. 5(f), there is still a rough structure of nanometer scale. Compared with the two groups of micro-graphs, it can be found that the surface of the circuit board treated by superhydrophobic coating has a better rough
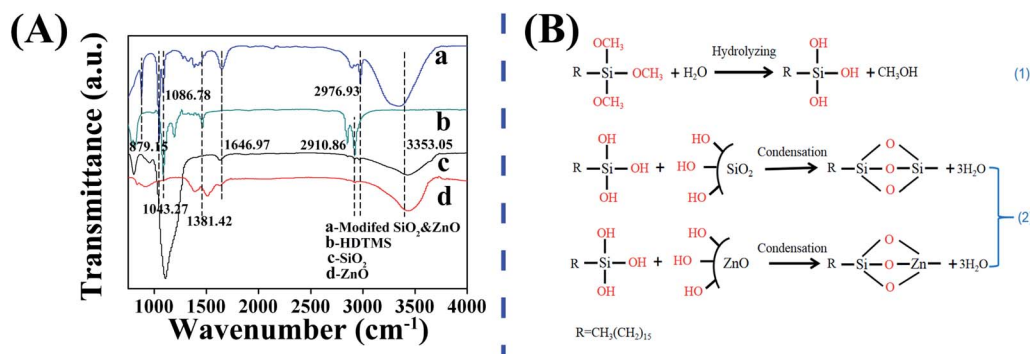

Fig. 4   FTIR spectra of different samples (A); possible reaction mechanism of HDTMS modified nanoparticles (B).
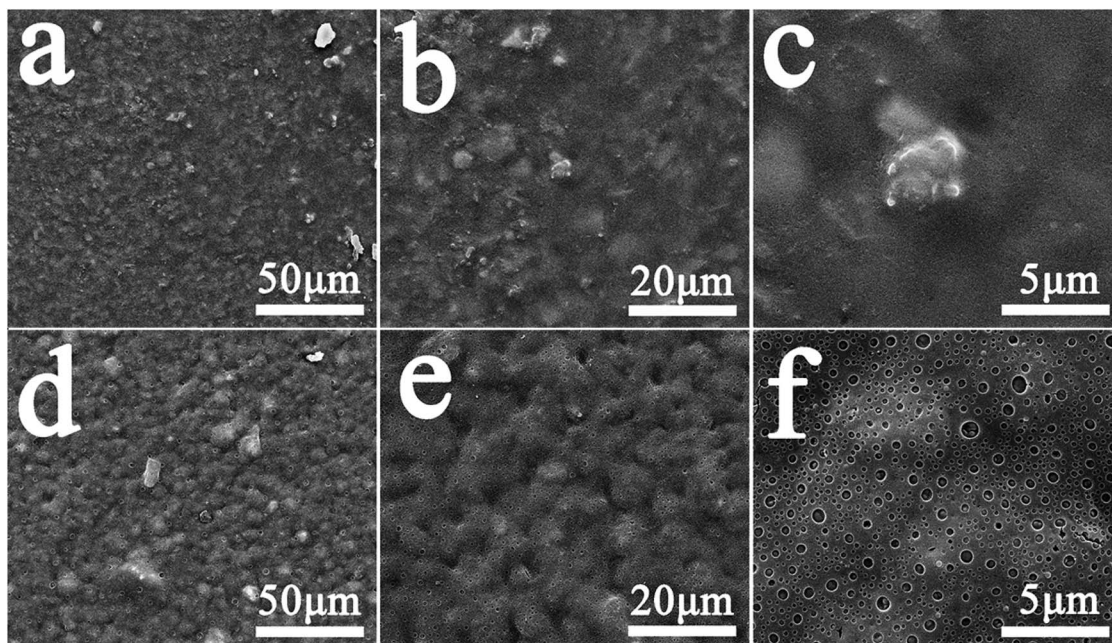
Fig. 5 SEM of pristine PCB surface (a–c); SEM of superhydrophobic PCB surface (d–f).

structure, so it has a better hydrophobicity. It can be found from Table 1 that the content of C, N, Si and Zn in the circuit board treated by superhydrophobic coating is obviously increased, especially Si and Zn, this is corresponding to the element content of HDTMS used in the modification of nanoparticles, which further indicates that the nanoparticles are successfully mixed into the coating and the grafting of HDTMS is successful.

3.2. Stability analysis

3.2.1. Corrosion resistance.
Electronic equipment in the process of using will encounter some harsh environment, such as acid rain, sea water, *etc.*, these bad factors will corrode the circuit board, so the circuit board has good corrosion resistance is very necessary. The samples were soaked in aqueous solutions with different pH values or NaCl (3.5 wt%) aqueous solutions, and then washed and dried with water at intervals. The changes of surface wettability of the samples were recorded. The wettability relationship of samples immersed in aqueous solutions with different pH values for 12 h is shown in Fig. 6(A), the wettability of the sample immersed in NaCl (3.5 wt%) solution for different time is shown in Fig. 6(B), the Nyquist plots of bare Cu samples, superhydrophobic samples and

superhydrophobic samples soaked in NaCl (3.5 wt%) solution for different times are shown in Fig. 6(C).

It can be seen from Fig. 6(A), the dramatic changes in both parameters are observed within the whole pH scale, particularly in the strong acid (1–5) and alkali (9–12) ranges. However, even after 12 h of soaking in the aqueous solutions with pH values of 1 and 12, the contact angle can still reach the values of 153°–154°, whereas the sliding angles may strongly deviate from the references. In the case of pH 5–9, the contact angle is greater than 150° and the sliding angle is less than 10°. Therefore, coatings remain superhydrophobic and exhibit good resistance to acids and alkalis at pH of 5–9, thus allowing the circuit boards to be applied within this pH range.

Both wettability parameters were found to undergo drastic changes with increasing soaking time in NaCl aqueous solutions: whereas the contact angle decreased from 169.9° to 149.6°, the sliding angle rose from 2.2° to 34.5°. It can be seen from Fig. 6(B) that the contact angle decreased by about 6° and the sliding angle increased by 6° after 48 h of soaking. After 144 h, the static contact angle was 152.3°, still achieving the superhydrophobic effect, and the sliding angle increased to 29.8°. With the increase of time, Na^+ and Cl^- begin to destroy the waterproof barrier of superhydrophobic coating, invade into the coating, and then destroy the sample. On the whole, the sample has good stability in NaCl aqueous solutions.

It can be seen from Fig. 6(C) that the charge transfer impedance of the superhydrophobic sample is about 10 000 times that of the bare Cu sample, the results show that the superhydrophobic coating has good corrosion resistance. With the increase of immersion time in NaCl (3.5 wt%) aqueous solutions, the charge transfer impedance of the sample decreases, but it still has good corrosion resistance compared with the bare Cu sample.

Table 1 EDS comparison between pristine and superhydrophobic PCB

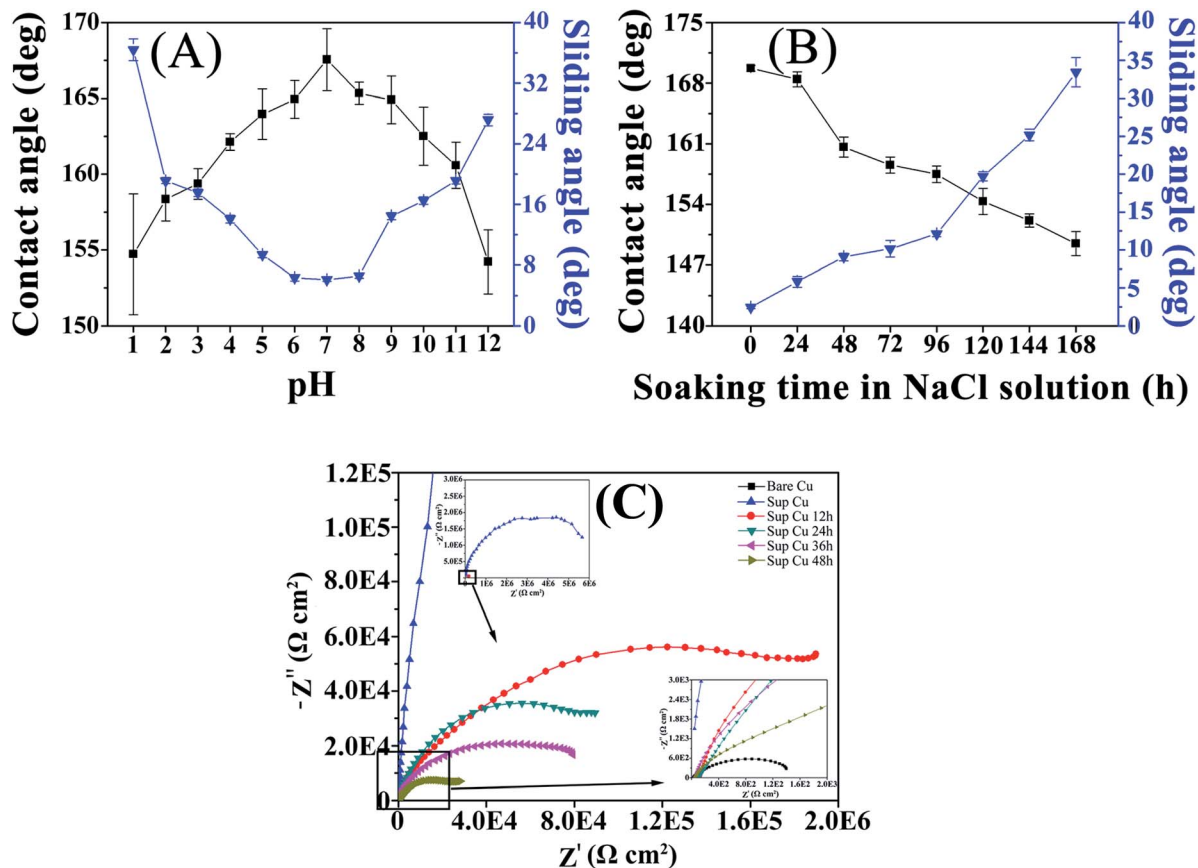| Element wt%	Pristine PCB	Superhydrophobic PCB
C	53.49	59.46
N	03.05	04.65
O	09.94	04.37
Si	01.19	02.73
Zn	00.06	00.63

Fig. 6 Wettability diagram of samples soaked in different pH aqueous solutions for 12 h (A); wettability of samples immersed in NaCl (3.5 wt%) aqueous solutions for different time (B); Nyquist plots of different samples (C).

The reason why the samples have good corrosion resistance is that the superhydrophobic coating has low surface energy and repels the solution. At the same time, air can be stored in the surface of a nano-rough structure, forming an air layer, thus protecting the circuit board from the exposure of other corrosive media. Since superhydrophobicity itself is the physical barrier against NaCl aqueous solutions immersion. The synergistic effect of the above three aspects enhanced the corrosion resistance of the samples.

3.2.2. Wear resistance test of coating. The relationship between friction times and wettability of samples is shown in

Fig. 7(A) and (B) shows SEM after 50 times wear of samples on 800 mesh sandpaper.

It can be seen from Fig. 7(A) that both the contact angle and sliding angle noticeably vary within the entire friction time range. The contact angle of the coating decreases with increasing wear time. When the wear time reaches 40, the contact angle is still at the expected level (151.47°), showing the good superhydrophobicity. Fig. 7(B) shows the SEM of samples with different magnification after 50 times of friction. The coating surface friction marks, a portion of the coating was off, but still part of the coating is preserved, can be seen in Fig. 7
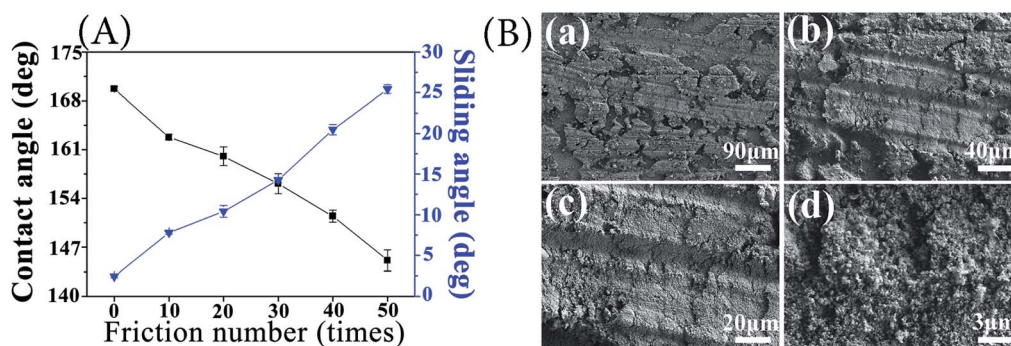

Fig. 7 Relationship between friction times and wettability of samples (A); SEM of the worn surface of the sample for 50 times (B).
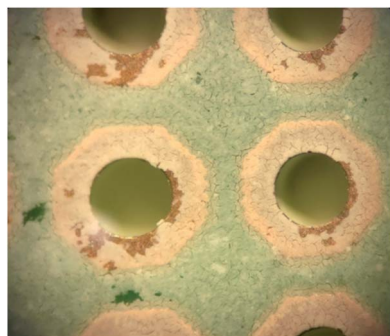
Fig. 8 Sample magnification 50 times.

[B(d)] at high magnification is still has many nanoscale rough structure, sample has good friction resistance.

3.3. Application analysis: mildew resistance and self cleaning performance

The results of this sample under GB/T 2423.16-2008. It can be found from Fig. 8 that no obvious long mildew was found under 50 times magnification, and the mould resistance level reached grade 0, which indicated that the sample had good mildew resistance. The surface layer of superhydrophobic coating is composed of SiO_2 and ZnO nanoparticles, when ZnO is in contact with mildew, ZnO can produce Zn^{2+}, which can combine with organic matter in mildew, destroy its internal structure, cause cell damage, and achieve antimildew effect. This is the chemical mechanism of antimildew of samples. The surface of superhydrophobic coating is micro–nano rough structure, and the air can be stored in the micro–nano rough structure to form an air layer, which can prevent mildew from adhering to and immersing in the sample. This is the physical mechanism of mildew resistance of the sample. The cooperation of the above two mechanisms makes the samples have good mildew resistance.

Fig. 9 shows the self-cleaning performance of the sample by simulating dust with cement powder. The sample is tilted at 10° and the water drops slowly from 1 cm away from the sample surface through the dropper at the higher end of the sample. It is found that the water droplets will automatically adhere to the passing dust during the rolling process of the super-hydrophobic PCB surface, so as to take away all the dust on the path. The water droplets are dry and clean on the rolling path,

and there is neither residual dust nor adhesive water droplets, showing a good self-cleaning effect. However, water droplets will agglomerate with dust on the pristine PCB surface, which cannot achieve the effect of self-cleaning.

4. Conclusions

The nano particles were modified by hexadecyl trimethoxysilane. The modified nano particles were compounded with silica sol, and then prepared by one-step spray method SiO_2 & ZnO/silica sol composite superhydrophobic coating. The effects of the mass ratio of SiO_2 to ZnO, the mass ratio of surface modifier to nanoparticles, and the mass ratio of nanoparticles to silica sol on the hydrophobicity of the coating were investigated. The results show that when the mass ratio of SiO_2 to ZnO is 2 : 1, the mass ratio of surface modifier to nanoparticles is 4.5%, and the mass ratio of nanoparticles to silica sol is 5%, the superhydrophobic coating has the best hydrophobicity, the contact angle can reach 169.47° and the sliding angle can reach 1.2°. The superhydrophobic coating has good mildew resistance, corrosion resistance, friction resistance and self-cleaning performance.

Conflicts of interest

There are no conflicts to declare.

Acknowledgements

References

1 X. Wang, Y. Guo, Ji. Liu, Q. Qiao and J. Liang, PVC-based composite material containing recycled non-metallic printed circuit board (PCB) powders, *J. Environ. Manage.*, 2010, **91**, 2505–2510.

2 S. Rajesh, V. Nisa, K. Murali and R. Ratheesh, Microwave dielectric properties of ptfe/rutile nanocomposites, *J. Alloys Compd.*, 2009, **477**, 677–682.

3 S. Wan, Y. Cong, D. Jiang and Z. Dong, Weathering barrier enhancement of printed circuit board by fluorinated silica based superhydrophobic coating, *Colloids Surf., A*, 2018, **538**, 628–638.

4 J. Gao, X. Huang, L. Wang, N. Zheng, W. Li, H. Xue, R. Li and Y. Mai, Super-hydrophobic coatings based on non-solvent induced phase separation during electro-spraying, *J. Colloid Interface Sci.*, 2017, **506**, 603–612.

5 W. Huang and C. Lin, Robust superhydrophobic transparent coatings fabricated by a low-temperature sol–gel process, *Appl. Surf. Sci.*, 2014, **305**, 702–709.
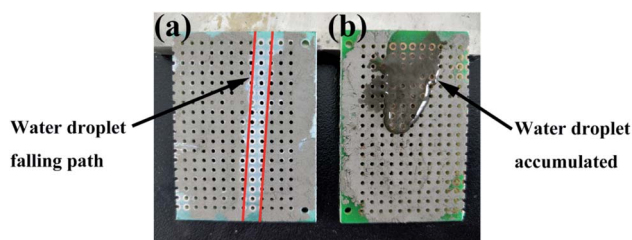
Fig. 9 Self cleaning properties of the superhydrophobic PCB as compared with the pristine PCB. Cement soils were washed away by the water droplets impacted onto the superhydrophobic PCB (a) and wetted by the water droplets impacted to the pristine PCB (b).

6 N. Wang and D. Xiong, Superhydrophobic membranes on metal substrate and their corrosion protection in different corrosive media, *Appl. Surf. Sci.*, 2014, **305**, 603–608.

7 A. Mulroney and M. Gupta, Optically transparent superhydrophobic polydimethylsiloxane by periodic surface microtexture, *Surf. Coat. Technol.*, 2017, **325**, 308–317.

8 E. Cho, C. Jian, H. Chen, K. Chuang, J. Zheng, Y. Hsiao, K. Lee and J. Huang, Robust multifunctional superhydrophobic coatings with enhanced water/oil separation, self-cleaning, anti-corrosion, and anti-biological adhesion, *Chem. Eng. J.*, 2017, **314**, 347–357.

9 D. Lv, N. Fang and W. Zhang, A PDMS modified polyurethane/Ag composite coating with super-hydrophobicity and low infrared emissivity, *Infrared Phys. Technol.*, 2020, **108**, 103351.

10 Z. Li, Y. Xing and J. Dai, Superhydrophobic surfaces prepared from water glass and non-fluorinated alkylsilane on cotton substrates, *Appl. Surf. Sci.*, 2008, **254**, 2131–2135.

11 A. A. Ahmad, Q. M. Al-Bataineh, A. M. Alsaad, T. O. Samara and K. A. Al-izzy, Optical properties of hydrophobic ZnO nano-structure based on antireflective coatings of ZnO/TiO/SiO thin films, *Phys. B*, 2020, **593**, 412263.

12 S. Zhang, X. Zheng, P. Wang and D. Zhang, Fabrication of super-hydrophobic micro-needle ZnO surface as corrosion barrier against corrosion in simulated condensation environment, *Colloids Surf., A*, 2020, **585**, 124087.

13 L. Jiang, Y. Zhao and J. Zhai, A Lotus-Leaf-like superhydrophobic surface: A porous microsphere/nanofiber composite film prepared by electrohydrodynamics, *Angew. Chem.*, 2004, **116**, 4435–4441.

14 J. Zhang and S. Seeger, Polyester materials with superwetting silicone nanofilaments for oil/water separation and selective oil absorption, *Adv. Funct. Mater.*, 2011, **21**, 4699–4704.

15 D. W. Wei, H. Wei, A. C. Gauthier, J. Song, Y. Jin and H. Xiao, Superhydrophobic modification of cellulose and cotton textiles: Methodologies and applications, *J. Bioresour. Bioprod.*, 2020, **5**, 1–15.

16 F. Guan, Z. Song, F. Xin, H. Wanl, D. Yu, G. Li and W. Liu, Preparation of hydrophobic transparent paper *via* using polydimethylsiloxane as transparent agent, *J. Bioresour. Bioprod.*, 2020, **5**, 37–43.

17 H. Zhou, H. Wang, H. Niu, A. Gestos, X. Wang and T. Lin, Fluoroalkyl silane modified silicone rubber/nanoparticle composite: A super durable, robust superhydrophobic fabric coating, *Adv. Mater.*, 2012, **24**, 2409–2412.

18 L. Feng, Z. Zhang, Z. Mai, Y. Ma, B. Liu, L. Jiang and D. Zhu, A super-hydrophobic and super-oleophilic coating mesh film for the separation of oil and water, *Angew. Chem.*, 2004, **43**, 2012–2014.

19 C. Hsu, L. Chang, C. Chiu, P. Lee and J. Lin, Facile fabrication of robust superhydrophobic epoxy film with polyamine dispersed carbon nanotubes, *ACS Appl. Mater. Interfaces*, 2013, **5**, 538–545.

20 A. Accardo, F. Gentile, F. Mecarini, F. Angelis, M. Burghammer, E. Fabrizio and C. Riekel, Ultrahydrophobic PMMA micro- and nano-textured surfaces fabricated by optical lithography and plasma etching for X-ray diffraction studies, *Microelectron. Eng.*, 2011, **88**, 1660–1663.

21 B. Bhushan, Y. Jung, A. Niemietz and K. Koch, Lotus-Like biomimetic hierarchical structures developed by the self-assembly of tubular plant waxes, *Langmuir*, 2009, **25**, 1659–1666.

22 X. Han, J. Peng, S. Jiang, Y. Song and X. Gong, Robust Superamphiphobic Coatings Based on Raspberry-like 2 Hollow SnO₂ Composites, *Langmuir*, 2020, **36**(37), 11044–11053.

23 J. Zhang, L. Zhang and X. Gong, Large-Scale Spraying Fabrication of Robust Fluorine-Free Superhydrophobic Coatings Based on Dual-Sized Silica Particles for Effective Antipollution and Strong Buoyancy, *Langmuir*, 2021, **37**(19), 6042–6051.

24 Q. Li, Y. Yan, M. Yu, B. Song, S. Shi and Y. Gong, Synthesis of polymeric fluorinated sol–gel precursor for fabrication of superhydrophobic coating, *Appl. Surf. Sci.*, 2016, **367**, 101–108.

25 A. Coclite, Y. Shi and K. Gleason, Super-Hydrophobic and oleophobic crystalline coatings by Initiated chemical vapor deposition, *Phys. Procedia*, 2013, **46**, 56–61.

26 D. Li, H. Wang, Y. Liu, D. Wei and Z. Zhao, Large-scale fabrication of durable and robust super-hydrophobic spray coatings with excellent repairable and anti-corrosion performance, *Chem. Eng. J.*, 2019, **367**, 169–179.

27 C. Li, Y. Sun, M. Cheng, S. Sun and S. Hu, Fabrication and characterization of a TiO2/polysiloxane resin composite coating with full-thickness super-hydrophobicity, *Chem. Eng. J.*, 2018, **333**, 361–369.

28 P. Wang, M. Chen, H. Han and X. Fan, Transparent and abrasion-resistant superhydrophobic coating with robust self-cleaning function in either air or oil, *Prog. Org. Coat.*, 2020, **146**, 105700.

29 Z. Liang, W. Li, B. Dong, Y. Sun, H. Tang, L. Zhao and S. Wang, Double-function SiO₂-DMS coating with antireflection and superhydrophobic surface, *Chem. Phys. Lett.*, 2019, **716**, 211–214.

30 Q. Su, F. Wen, Y. Huang and B. Wang, Abrasion resistant semitransparent self-cleaning coatings based on porous silica microspheres and polydimethylsiloxane, *Ceram. Int.*, 2019, **45**, 401–408.

31 B. Xu, Y. Huang and B. Wang, Preparation and performance of fluorine-free superhydrophobic coatings based on modified silica and polysiloxane, *Fine Chem.*, 2019, **36**, 2009–2015.

32 J. Ou, F. Wang, W. Li, M. Yan and A. Amirfazli, Methyltrimethoxysilane as a multipurpose chemical for durable superhydrophobic cotton fabric, *Prog. Org. Coat.*, 2020, **146**, 105700.

33 X. Wei, N. Li, W. Yi, L. Li and Z. Chao, High performance super-hydrophobic porous ceramic coating with flower-like CeO₂ micro/nano-structure, *Surf. Coat. Technol.*, 2017, **32**, 565–571.